Jour. Geol. Soc. India (2022) 98:431-439
https://doi.org/10.1007/s12594-022-1996-z

ORIGINAL ARTICLE

Study on Seismic Amplification Effect and Active Earth Pressure of Retaining Wall Based on Pseudo-Dynamic Method and Numerical Simulation

Yahong Deng[1,2], Zuofei Yan[1,3*], Nainan He[1], Jiang Chang[1] and You Xuan[1]

[1]Department of Geological Engineering, Chang'an University, Xi'an 710064, China
[2]Key Laboratory of Mine Geological Hazards Mechanism and Control, Xi'an 710054, China
[3]Beijing General Municipal Engineering Design & Research Institute Co., Ltd., Beijing 100082, China
***E-mail:** 343951033@qq.com*

Received: 6 January 2021 / Revised form Accepted: 6 May 2021

ABSTRACT

In this paper, the finite element numerical analysis verified that the critical failure surface of the backfill under active conditions was curved, and it was consistent with the composite form of a logarithmic spiral and a straight line assumed by the study based on the pseudo-dynamic method. On the basis of the failure surface of the backfill as a curved surface, the seismic active earth pressure on the retaining wall was calculated by the pseudo-dynamic method and the finite element method respectively. Results showed that in the finite element analysis, the acceleration amplitude of the backfill had an obvious amplification effect along the depth of the retaining wall, and this amplification effect was related to many factors. Under the action of low-frequency seismic load, linear amplification effect occurred, while nonlinear amplification effect occurred under the action of high-frequency seismic load. The amplification factors increased with the increase of retaining wall height. According to the characteristics of the amplification effect, after modifying the input seismic acceleration in the pseudo-dynamic method, the distribution of seismic active earth pressure on the retaining wall was close to that obtained by finite element analysis.

INTRODUCTION

As a kind of structure to maintain the stability of rock and soil mass, retaining wall was widely used in geotechnical engineering. In seismic design of retaining wall, the main consideration factors were the total earth thrusts and the distribution characteristics of the earth pressure on retaining walls. In simple terms, the total earth thrust was the incentive for the retaining wall to slip, and the distribution of earth pressure determined the position of action point of the total thrust, which was the reason for the overturning destruction of the retaining wall. Therefore, it was of great practical significance to determine the active earth pressure on the retaining wall under seismic condition. Many experts and scholars had used experiments, theoretical derivation and numerical analysis to obtain the active earth pressure on the retaining wall under seismic condition. Based on static Coulomb earth pressure theory, Okabe (1924) and Mononobe and Matsuo (1929) conducted in-depth investigations on different forms of retaining wall failure modes during earthquakes and proposed equations for the calculation of seismic earth pressures on retaining walls, known as Mononobe-Okabe (M-O) or pseudo-static method. Seed and Whitman (1970) modified M-O method and it had been widely recognized and applied. They divided the total earth pressure on the retaining wall under seismic condition into static earth pressure and dynamic earth pressure, and believed that the dynamic earth pressure was distributed along the retaining wall in an inverted triangle and the action point was located at 0.6H from the bottom of the wall. In this way, the overturning moment of the retaining wall calculated was greater than that of the M-O method. The pseudo-static method considered seismic load as a simple inertial force to take into account the dynamic nature of earthquake loadings in a very approximate way. Steedman and Zeng (1990) proposed a pseudo-dynamic method to consider certain dynamic response characteristics in a relatively simple way. Their proposed method solved the problem of seismic earth pressure by taking into account the phase differences and amplification effects of seismic waves, which assumed the critical fracture surface of the backfill as being planar. Zeng et al. (1993) verified the rationality of the pseudo-dynamic analysis results by comparing the centrifuge model experiment with the theoretical analysis results. In the pseudo-dynamic method proposed by Steedman and Zeng (1990), simply shear wave velocity (v_s) and horizontal seismic acceleration ($k_h g$, where g is the acceleration due to gravity) were considered. Choudhury and Nimbalkar (2006) considered primary wave velocity (v_p) and vertical seismic acceleration ($k_v g$) based on the pseudo-dynamic method developed by Steedman and Zeng (1990) to study the seismic earth pressures on retaining walls. Many other researchers have conducted detailed studies using pseudo-dynamic method, assuming the failure surface of the backfill to be planar (Ghosh, 2010; Ghosh and Sharma, 2011; Bellezza, 2015; Maskar et al., 2017; Rajesh and Choudhury, 2017).

All above mentioned methods assume the failure surface of backfill to be planar. Terzaghi (1943) found that the seismic earth pressure coefficients obtained by assuming flat failure surfaces had large deviations from real values with calculation errors of up to 3 times higher than the real value. Kramer (1996) had articulated the presence of shear stresses on the wall-soil interface can shift the position of major principal stress axis near the back of the wall. If the inclination of the principal stress axes varies within the backfill, the inclination of the failure surface must also vary. The failure surface of the backfill was assumed to be a combination of a logarithmic spiral and a straight

line. By assuming curved failure surfaces, Kumar (2001) deduced theoretical equations for the calculation of seismic earth pressures on the back of inclined retaining walls based on pseudo-static method. It was found the calculated seismic earth pressures were more reasonable when the critical failure surface was assumed to be curved. Based on pseudo-static method, Soubra and Abdul-Hamid (2001), Choudhury (2004), and Subba Rao and Choudhury (2005) assumed critical failure surfaces as logarithmic spiral or a combination of logarithmic spiral and straight lines and derived theoretical equations for seismic earth pressures at different dip angles of retaining walls. Also, Basha and Babu (2009, 2009, 2010, 2010) studied seismic structures using pseudo-dynamic method by assuming curved critical failure surface for backfill, but did not obtain the distributions of seismic earth pressures along the depth of retaining walls. Xu et al. (2015) applied the LSR (Log-Spiral-Rankine) model to assess active and passive seismic earth pressures and introduced local and global iteration schemes to solve the resulting highly coupled multivariate nonlinear system of equations, which was more complicated. Santhoshkumar et al. (2019) computed the seismic active resistance of a slanted cantilever retaining wall holding a cohesionless backfill and did not assume a preordained failure mechanism.Then Yan et al. (2020), on the basis of pseudo-dynamic method, assumed that the critical failure surface of the backfill was a composite surface in the form of a logarithmic spiral and a straight line. They deduced seismic active earth pressure and its distribution characteristics on the retaining wall according to the limit equilibrium theory, and compared the results with existing methods.

Experimental methods and numerical analysis are often needed to verify and compare the theoretical results. Nakamura and Shinya (2006) carried out centrifuge model test and obtained seismic earth pressure data on the retaining wall, which was verified and compared with the theoretical method results of Mononobe-Okabe. They found that M-O method could not truly reflect the earth pressure characteristics of retaining wall under seismic condition. Miriano et al. (2016) used ABAQUS finite element numerical simulation software and two different constitutive model materials to study the earth pressure on flexible retaining wall under seismic load. Junied and Mohd (2018) used the hardening soil constitutive model in PLAXIS2D finite element software to calculate the seismic earth pressure of retaining wall. They compared the calculated results with the results of centrifuge tests implemented by Okamura, Matsuo (2002) and Nakamura (2006). Jo et al. (2017) designed and implemented two groups of centrifuge model test to study total earth thrust and earth pressure distribution characteristics on cantilever retaining wall. The test results were compared with M-O method and S-W method. And they found that the spectrum characteristics of the input ground motion affects the phase difference of the backfill and the retaining wall, thus affects the seismic earth pressure. Tavakoli et al. (2019) used PLAXIS finite element analysis software and Mohr-Coulomb constitutive model (elastic-perfectly plastic model) to study the amplification effect of seismic acceleration, which was generated by backfill from many factors. However, the Mohr-Coulomb constitutive model, as a simple elastic-perfectly plastic model, cannot well reflect the dynamic characteristics of the backfill soil. So it is not suitable for the real dynamic nonlinear constitutive material model.

METHOD OF ANALYSIS

In this paper, based on the curved critical failure surface of the backfill, the pseudo-dynamic method and the finite element method were used to compare and study the magnitude and distribution characteristics of the seismic active earth pressure on the retaining wall. The calculation method used in the pseudo-dynamic method was similar to that used by Choudhury and Nimbalkar (2006). The soil wedge was divided into horizontal thin elements for a series of calculus operations but the difference lies mainly in the form of failure surface. In the analysis process, the amplification effect of acceleration amplitude and its causes were mainly studied, and the input seismic acceleration in pseudo-dynamic method was modified according to the amplification effect characteristics obtained by numerical analysis. The results of pseudo-dynamic method and numerical analysis method were compared with those of Mononobe-Okabe method, Choudhury and Nimbalkar method.

Pseudo-dynamic Method

The calculation model of a typical gravity retaining wall in the pseudo-dynamic method adopted in this study is shown in Fig. 1. The back of the retaining wall was vertical with the height of *H*, and the backfill was non-cohesive. The influences of amplification factor, soil friction angle, soil-wall friction angle, horizontal and vertical acceleration coefficients were considered. Under the action of horizontal and vertical seismic forces, the horizontal and vertical

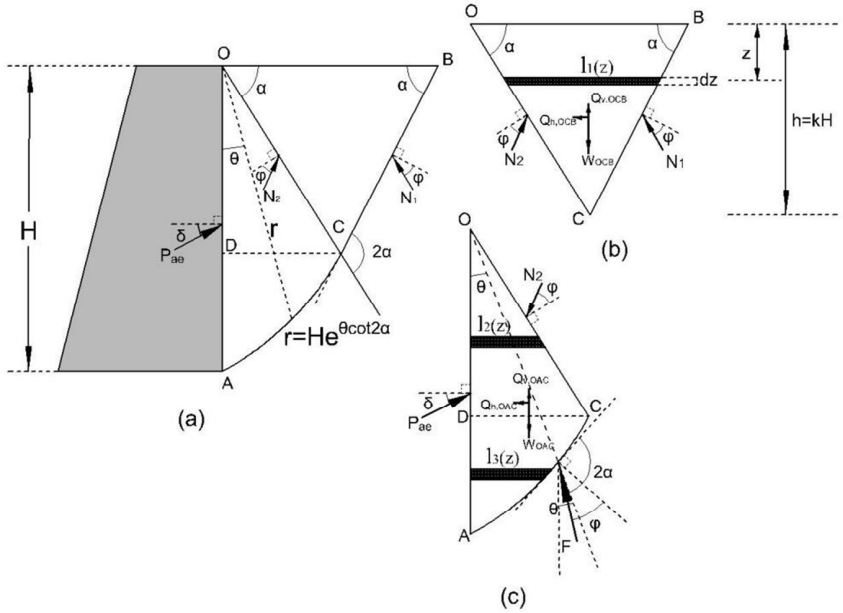

Fig. 1. Schematic diagram of retaining wall calculation model (where (a) is the overall calculation model, (b) and (c) represent the failure wedges *OCB* and *OAC*)

acceleration by earthquakes in any depth z and time t were:

$$a_h(z,t) = F_a(z)k_h g \sin\omega\left(t - \frac{H-z}{v_s}\right) = F_a(z)k_h g \sin 2\pi\left(\frac{t}{T} - \frac{H-z}{\lambda_s}\right) \quad (1)$$

$$a_v(z,t) = F_a(z)k_v g \sin\omega\left(t - \frac{H-z}{v_p}\right) = F_a(z)k_v g \sin 2\pi\left(\frac{t}{T} - \frac{H-z}{\lambda_p}\right) \quad (2)$$

According to the principles of pseudo-dynamic method, the following basic assumptions were adopted:

a. The retaining wall was rigid, the back of the wall was vertical, and the surface of the backfill is horizontal;
b. The critical failure surface of the backfill (as shown in Fig.1) was a composite curved surface in the form of a logarithmic spiral and a straight line;
c. Backfill was homogeneous, isotropic, dry, and non-cohesive soil.

The specific force analysis and derivation process of the pseudo-dynamic method studied in this paper were detailed in Yan et al. (2020), which would not be repeated here. And the total active thrust under seismic conditions could be obtained as:

$$P_{ae}(t) = \frac{1}{\cos(2\alpha-\delta-\phi)+\sin(\alpha-\delta-\phi)} \times \begin{Bmatrix} N_2(t)[\sin(3\alpha-2\phi)-\cos(2\alpha-2\phi)] \\ +(W_{OAC}-Q_{v,OAC}(t))[\sin(2\alpha-\phi)-\cos(\alpha-\phi)] \\ +Q_{h,OAC}(t)[\sin(\alpha-\phi)+\cos(2\alpha-\phi)] \end{Bmatrix} \quad (3)$$

The distribution of seismic active earth pressure was obtained by differentiating total active thrust $P_{ae}(t)$ as:

$$p_{ae}(t) = \frac{\partial P_{ae}(t)}{\partial z} = \frac{1}{\cos(2\alpha-\delta-\phi)+\sin(\alpha-\delta-\phi)} \times \begin{Bmatrix} \frac{\partial N_2(t)}{\partial z}[\sin(3\alpha-2\phi)-\cos(2\alpha-2\phi)] \\ +(\frac{\partial W_{OAC}}{\partial z}-\frac{\partial Q_{v,OAC}(t)}{\partial z})[\sin(2\alpha-\phi)-\cos(\alpha-\phi)] \\ +\frac{\partial Q_{h,OAC}(t)}{\partial z}[\sin(\alpha-\phi)+\cos(2\alpha-\phi)] \end{Bmatrix} \quad (4)$$

Finite Element Method

The GTS NX finite element software was used for numerical analysis. The size of retaining wall, the divisions of computation mesh and the position of the monitoring points were as shown in Fig. 2. The free field boundary was selected for left and right sides of the boundary, which can absorb the reflection or refraction seismic waves from inside the system so as to eliminate the influence of the secondary reflection waves on the calculation results.

In order to simulate the dynamic response of the backfill and the foundation soil under seismic conditions, it is very important to select the material constitutive model rationally. considering the hysteresis loop of soil elements under loading and unloading, the attenuation characteristic of soil shear modulus, the damping characteristic of soil and so on. The constitutive model used in this study was the hardening soil model (considering the small strain effect), or "HSsmall Model" for short. Fig. 3 shows the loading and unloading stress-strain curves of a typical hardening soil model (Bakr and Ahmad, 2018).

Considering the damping of the material in the model, Rayleigh damping was adopted in this study, and its equation is as follows:

$$C = \alpha M + \beta K \quad (5)$$

Where C is the damping matrix, M and K are the mass and stiffness matrices respectively, $\acute{a}$ and $\hat{a}$ represent the Rayleigh damping coefficients, which are proportional to the mass and stiffness respectively and are calculated by:

$$\alpha + \beta\omega_i^2 = 2\omega_i \xi_i \quad (6)$$

Where ξ_i is the critical damping ratio. In almost all geological materials, the critical damping ratio is 0.05, so as in this study. And $\omega_i$is the natural vibration circle frequency in the two vibration modes, which can be obtained by eigenvalue analysis in GTS NX (Noorzad and Omidvar, 2010; Castaldo and Iuliis, 2014; Tavakoli et al., 2014a,b).

In this study, considering the comparison between the pseudo-dynamic method and the finite element method, the input seismic wave was a simple harmonic wave that was consistent with the pseudo-dynamic method (the frequencies, seismic acceleration coefficients, and ratios of the wall height to wavelength are equal or approximate). In order to study the characteristics of amplification effects of the backfill, 11 history monitoring points were arranged along the height of the retaining wall (as shown in Fig. 2).

Determination of Active Earth Pressure State

The pseudo-dynamic method used in this study, once the assumed failure surface was determined, considered that the calculation process is under the state of seismic active earth pressure. As for the finite element numerical simulation, the active earth pressure state of the retaining wall under seismic conditions was complicated and difficult to determine. The solution given in this study was to set the calculation model as the active earth pressure state of the retaining wall under the

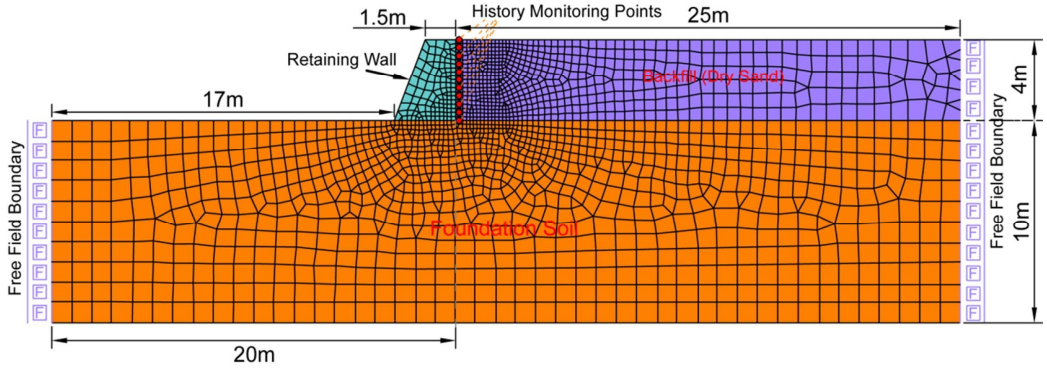

Fig.2 Modeling and finite element net.

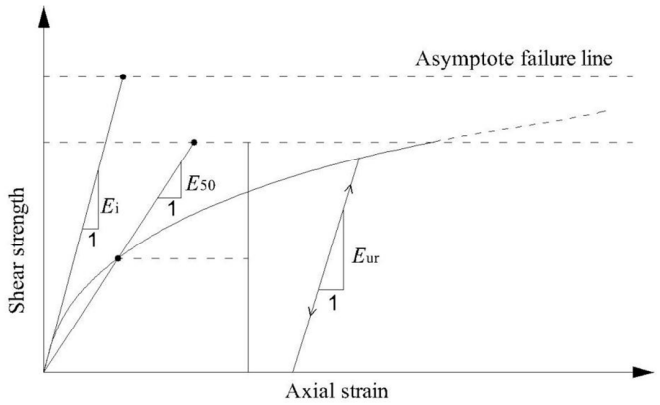

Fig. 3. Stress-strain relationship from a typical soil strength test.

static condition, and then input seismic waves for time-history analysis. Under static conditions, the constitutive model of backfill was first set as the Mohr-Coulomb constitutive model when certain wall and soil material parameters had been determined. In this way, the equivalent plastic zone of backfill could be obtained intuitively. If the plastic zone did not penetrate the wall heel and the ground surface, the unit weight of retaining wall would be reduced. After multiple times of unit weight reduction calculation, until the plastic zone of the backfill just penetrated the wall heel and the ground surface. The initial parameters of retaining walls, soil and other materials used in this study are shown in Table 1.

The present study did not consider the influence of foundation soil on the whole computing process. In the static analysis, the model of the foundation soil was set to the most simple elastic constitutive model, and in the dynamic analysis, due to the elastic material of amplification effect too large, the material of the foundation soil was the same as the backfill. Fig. 4 shows the comparison between the plastic zone form of the backfill under the static active earth pressure condition obtained by the finite element analysis and the failure surface form assumed by the pseudo-dynamic method. It could be concluded from the figure that, when the retaining wall was in the active limit equilibrium state under the static condition, the plastic zone of the backfill was curved instead of plane. Therefore, it was more reasonable to calculate the earth pressure by the pseudo-dynamic method when the failure surface was assumed to be a composite surface than when the failure surface is assumed to be plane.

RESULTS AND DISCUSSION

Amplification Effect of Backfill Soil

After the static active earth pressure state of the retaining wall was determined, the values of the original basic parameters remained unchanged. And then the constitutive model of the backfill would be replaced as HSsmall model. Before the dynamic analysis, the eigenvalue was first analyzed to obtain the natural vibration period T of the backfill, and then the shear wave velocity v_s=199 m/s could be calculated according to the formula $v_s = 4H/T$. Simple harmonic loads with acceleration amplitude of 0.1g, 0.2g, 0.3g and 0.4g were applied to the bottom of the model, and the frequency f varied from 0.5Hz to 40Hz on the calculation. Figure 5 shows the time-history curves of horizontal acceleration at each monitoring point (Fig. 2) after dynamic analysis. The vibration amplification factors can be calculated by dividing the amplitude of acceleration at each monitoring point by the amplitude of acceleration at the monitoring point at the bottom of the retaining wall.

According to Fig. 5, we could see that at low frequencies, the retaining wall height range, the time-history curves of horizontal acceleration were consistent in amplitude and phase (Fig. 5 a). With the increase of frequency, these curves had obvious differences in amplitude (Fig. 5 b), showing that the acceleration amplitude of backfill at the top position is the largest and that at the bottom is the smallest. After the frequency reached a considerable value (Fig. 5c and d), the time-history curves of horizontal acceleration of backfill at different depths along the height range of retaining wall were not only different in amplitude, but also significantly different in phase. The dynamic responses of harmonic seismic waves of different frequencies to the

Table 1 Soil and retaining wall properties and other parameters used for the present study

Parameter	Description	Unit	Value
Soil for M-C model			
γ_s	Unit weight	kN/m^3	19
E_s	Young's modulus	kPa	5×10^4
v_s	Poisson's ratio of sol	-	0.3
c	Cohesion	kPa	0
φ	Angle of internal friction	°	30
ψ	Dilatancy angle	°	5
Soil for HS model	(The basic parameters are identical with those in M-C model)		
p^{ref}	Reference confining pressure	kPa	100
E^{50}_{ref}	Modulus at 50% strength at failure, corresponding to p^{ref}	MPa	45
E^{50}_{oed}	*Modulus from an oedometer test, corresponding to* p^{ref}	MPa	45
E^{50}_{ur}	*Modulus for unloading-reloading conditions, corresponding to* p^{ref}	MPa	180
G^{ref}_0	*Initial small strain shear modulus, corresponding to* p^{ref}	MPA	168.5
$\gamma_{0.7}$	Reference shear strain, corresponding to G^{ref}_0	-	0.0002
R_f	*Failure ratio*	-	0.9
y	A constant, to account for the stiffness stress-level dependency	-	0.5
Retaining wall			
E_w	Young's modulus	MPa	30000
v_w	Poison's ratio of wall	-	0.15
γ_w	Unit weight	kN/m^3	24
Interface			
δ_{s-w}	*Soil wall friction angle*	°	15
δ_{f-w}	*Wall-foundation friction angle*	°	15
Kn_{s-w}	*Normal stiffness modulus of soil-wall interface*	kN/m^3	2×10^9
Kn_{s-f}	*Normal stiffness modulus of wall-foundation interface*	kN/m^3	2×10^9
Kt_{s-w}	*Shear stiffness modulus of soil-wall interface*	kN/m^3	2×10^9
Kt_{s-f}	*Shear stiffness modulus of wall-foundation interface*	kN/m^3	2×10^9

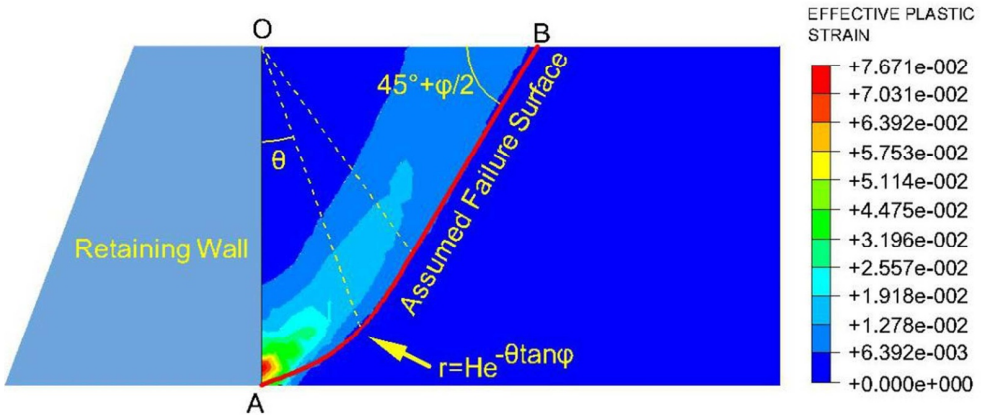

Fig.4 Comparison of the failure surface from the FE analysis and pseudo-dynamic method for the active case (when γ_w= 16.89 kN/m^3).

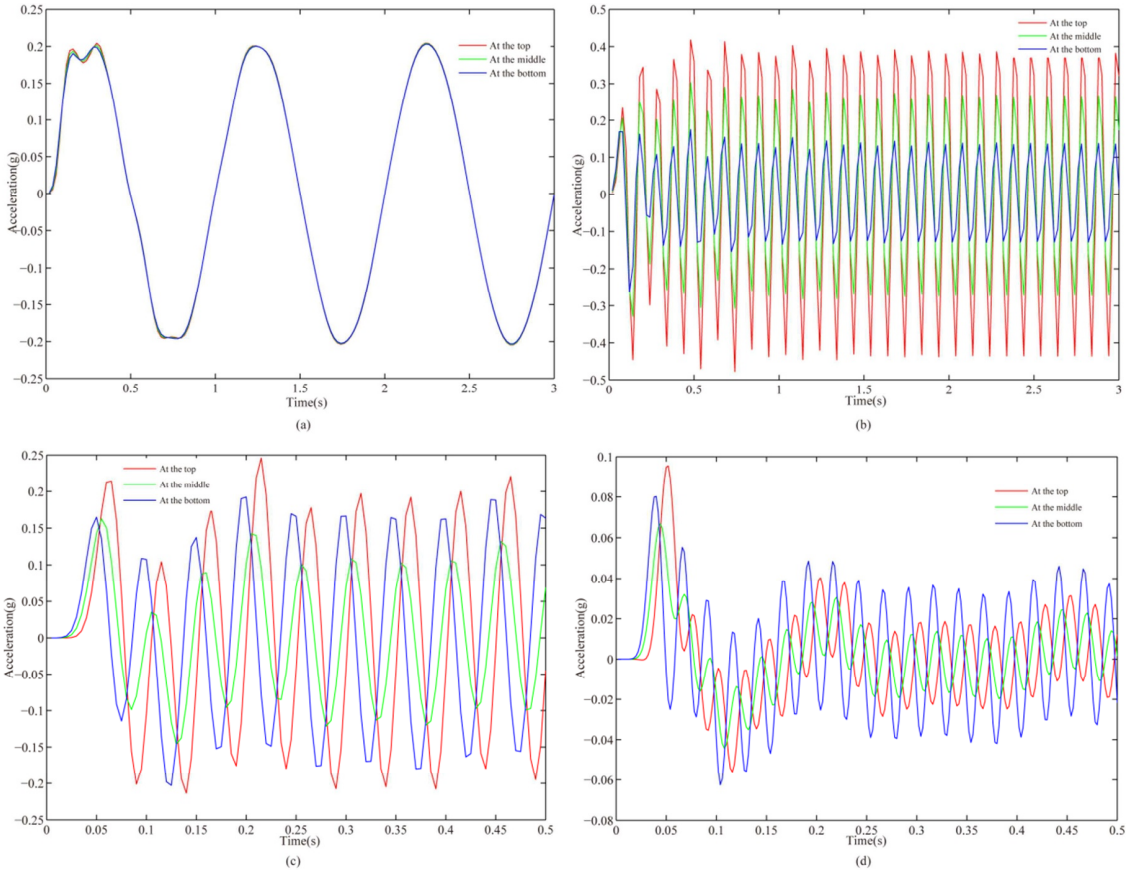

Fig.5. Horizontal acceleration time-history curves of partial monitoring points.(Where the amplitude of input simple harmonic wave is 0.2g and the frequencies are 1Hz, 10Hz, 20Hz and 40Hz in (a), (b), (c) and (d))

horizontal surface at the bottom of the retaining wall were different (mainly reflected in the amplitude of acceleration). In order to make the amplification effect intuitive and unified, the amplitude of acceleration of each monitoring point was divided by that at the bottom point , and the amplification factors of the backfill along the depth of the retaining wall were obtained.

Figure 6 shows the distributions of amplification factors along the depth range under the action of harmonic seismic waves with amplitude of 0.2g. It can be seen that at low frequency seismic waves (f < 5Hz), amplification factors has a linear distribution along the retaining wall, and the value of amplification factor is getting larger and larger from the bottom to the top. Under the action of high frequency (f>5Hz) seismic wave, the distributions of amplification factors are nonlinear. As shown in Fig. 7a, when the harmonic seismic wave acts on the backfill at a low frequency, the soil shows a nearly static response. And the low amplification factors indicate that the damping of soil does not significantly weaken the energy of seismic waves at low frequencies. With the increase of frequencies (Fig. 7b), the dynamic characteristics of soil are obvious. Due to the viscous damping of the material, the vibration amplification factors will increase or even decrease slightly when the seismic waves propagate to the ground surface. When the waves propagate to the surface, they will reflect, and the interaction of upward wave and downward wave is an important reason for the large increase of the amplification factors.

The larger the amplification factor is, the more unfavorable it is to the practical application of engineering. Therefore, in consideration of engineering safety design, we divided the amplification effects into

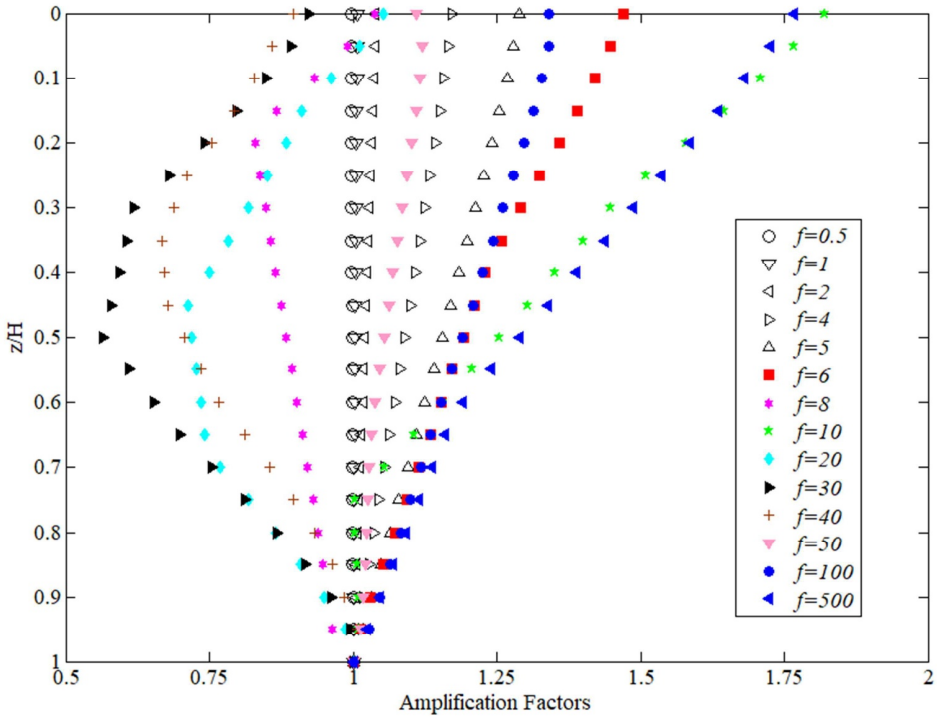

Fig.6. The distribution of the amplification factors along the depth of the retaining wall(Where the amplitude of input simple harmonic wave is 0.2g).

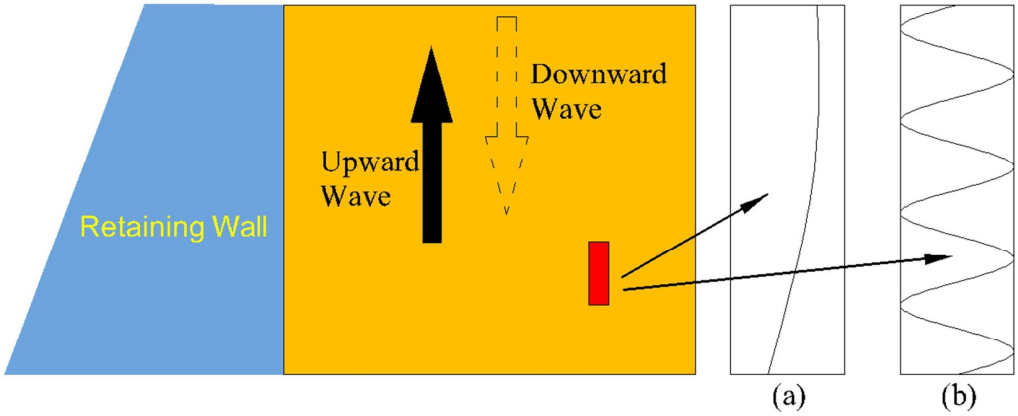

Fig.7 Simple diagram of high and low frequency seismic waves acting in the backfill elements.(The frequencies are 2Hz and 32Hz in (a) and (b).)

two parts: one is linear distribution of amplification factors at low-frequency seismic conditions, and the other is nonlinear distribution of amplification factors at high-frequency seismic conditions. According to Fig. 6, the low-frequency-linear distributions of amplification factors and the high-frequency-nonlinear distributions of amplification factors were separated, and the envelope lines connected along the maximum amplification factors along the retaining wall height is shown in Fig. 8. In this way, whether the distribution of amplification factors is linear or nonlinear, in the field of seismic safe design, the envelope line of distribution about amplification factors could be directly selected to conservatively calculate the total earth thrust and the distribution of earth pressure. Fig. 9 shows the influence of the amplitude of input acceleration on the distribution of amplification factors. Obviously, the amplification factors have little relationship with the amplitude of the input seismic wave. Fig. 10 shows the effect of the height of retaining wall on the distribution of amplification factors. It can be found that the higher the retaining wall is, the more obvious the amplification effect is and the larger the amplification factors are. However, the general characteristics of the distribution of amplification factors remain unchanged, that is, when the frequencies of seismic waves are less than 5Hz, the amplification factors present a linear distribution but when the frequencies are greater than 5Hz, the amplification factors present a nonlinear distribution.

Comparison between Pseudo-dynamic Method and Numerical Analysis

According to the above finite element numerical simulation results about the amplification factors, the linear and nonlinear amplification coefficient distributions could be fitted mathematically (as shown in Eq. (7)). This function takes into account both linear and nonlinear amplification factor distributions and the effect of height of retaining wall on the amplification factors. By substituting Eq. (7) into the seismic acceleration formulas Eqs. (8) and (9) to be input seismic accelerations in the pseudo-dynamic method and modifying them in the existing pseudo-dynamic method, the magnitude of total earth thrust and the distribution of earth pressure of the retaining wall could be calculated more reasonably according to the input seismic accelerations by using the pseudo-dynamic method.

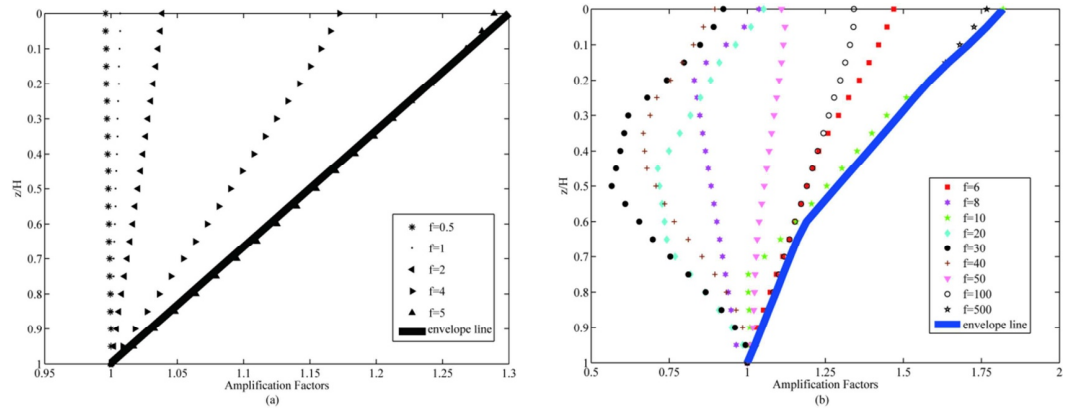

Fig.8. Distributions of amplification factors and its envelope lines.((a) for linear distributions and (b) for nonlinear distributions)

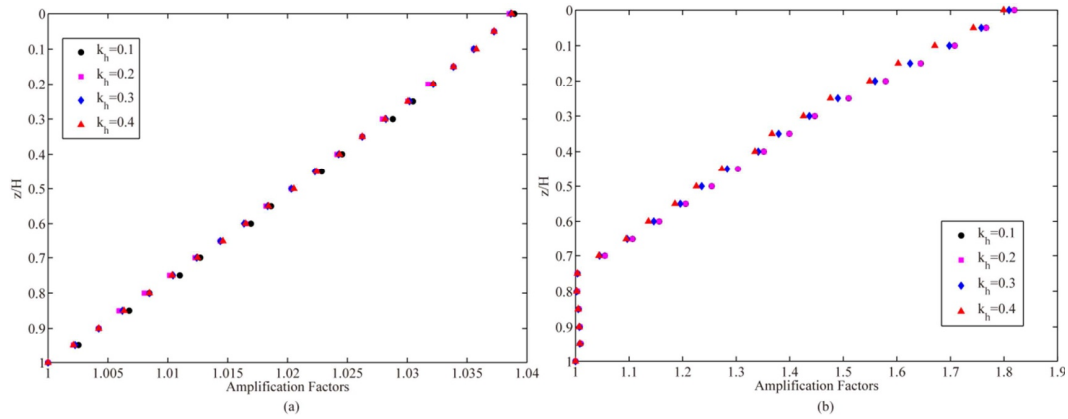

Fig.9 Effect of amplitude of seismic load on amplification factors.(The frequencies are 2Hz and 10Hz in (a) and (b) respectively)

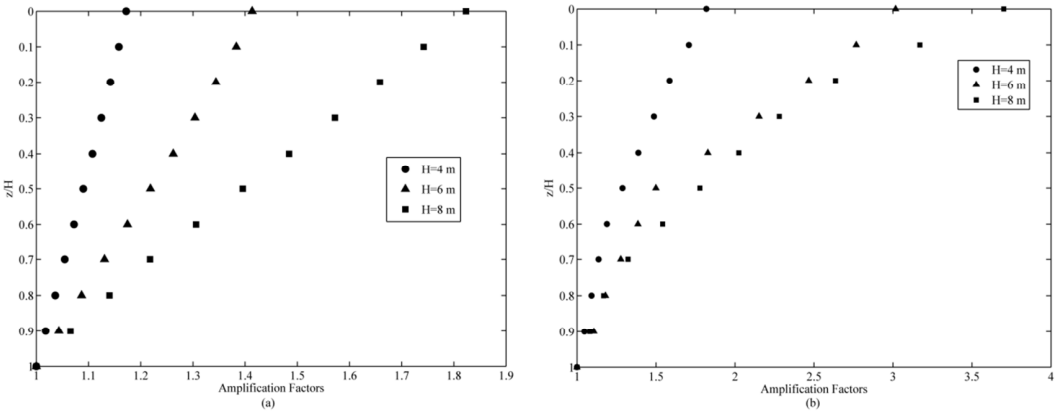

Fig.10 Effect of the height of retaining wall H on amplification factors.((a) for linear distributions and (b) for nonlinear distributions)

$$F_a(z)=\begin{cases}(0.02H^2-0.08H+1.18)*(1-0.15\dfrac{z}{H}) & f\le 5\\ (0.02H^2-0.08H+1.18)*[0.22(\dfrac{z}{H})^3+0.18(\dfrac{z}{H})^2-1.215(\dfrac{z}{H})+1.824] & f>5\end{cases} \tag{7}$$

Substitute Eq. (7) into the seismic acceleration formulas (like Eqs. (1) and (2)), we get

$$\begin{aligned}a_h(z,t)&=F_a(z)k_h g\sin\omega\left(t-\frac{H-z}{v_s}\right)\\&=F_a(z)k_h g\sin 2\pi\left(\frac{t}{T}-\frac{H-z}{\lambda_s}\right)\end{aligned} \tag{8}$$

$$\begin{aligned}a_v(z,t)&=F_a(z)k_v g\sin\omega\left(t-\frac{H-z}{v_p}\right)\\&=F_a(z)k_v g\sin 2\pi\left(\frac{t}{T}-\frac{H-z}{\lambda_p}\right)\end{aligned} \tag{9}$$

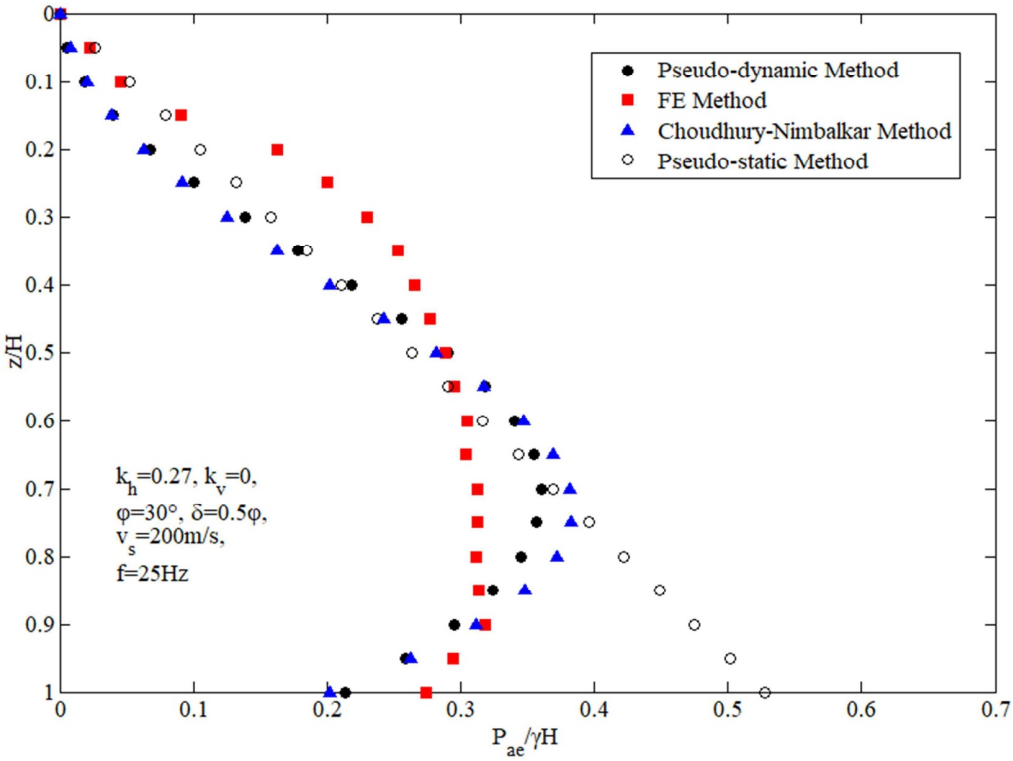

Fig.11. Comparison of seismic active earth pressure on retaining walls obtained by pseudo-dynamic method, FE method, C-N method and pseudo-static method (where $k_h = 0.27$, $k_v = 0$, $\varphi = 30°$, $\delta = 0.5\varphi$, $v_s = 200$ m/s, $f = 25$ Hz)

Eqs. (8) and (9) were substituted into Eq. (3) to calculate seismic total active earth thrust on the retaining wall based on the modified pseudo-dynamic method, which was then substituted into Eq. (4) to obtain the distribution of seismic active earth pressure on the retaining wall. Fig. 11 compared the distributions of seismic active earth pressure on retaining walls calculated by the proposed modified pseudo-dynamic method, FE method, C-N (Choudhury-Nimbalkar) method and pseudo-static method (M-O method). It can be seen from the figure that the distributions of seismic active earth pressure are nonlinear. As for the distribution form, the results obtained by the modified pseudo-dynamic method were similar to those obtained by the C-N method and slightly different from those obtained by the numerical analysis. It is calculated that there is a 1.6% difference in total earth thrust between the pseudo-dynamic method in this study and the C-N method and a 9.3% difference in total earth thrust between the pseudo-dynamic method and numerical analysis. In terms of the locations of the total earth pressure action points obtained according to the distributions, the action point calculated by pseudo-static method is located at 1/3*H* from the bottom of the retaining wall (*H* is the height of the retaining wall). The action point calculated by the pseudo-dynamic method in this study is 0.353*H* away from the bottom of the retaining wall. The action positions calculated by C-N method and finite element method are 0.344*H* and 0.387H away from the bottom of the retaining wall. In general, the comparison of seismic earth pressure on the retaining wall can be obtained as follows: pseudo-static method > FE method > C-N method > modified pseudo-dynamic method; Position of pressure action point: FE method > modified pseudo-dynamic method > C-N method > pseudo-static method. From the perspective of engineering practice, there are many factors affecting the active earth pressure of the retaining wall under seismic conditions, such as the interaction between the soil and the retaining wall under seismic load, the material characteristics of the retaining wall, and the deformation characteristics of the foundation soil. However, within a certain error tolerance range, the characteristics of seismic active earth pressure obtained in this study are nearly consistent with the results of the previous pseudo-static method, C-N method and the finite element method, which has certain guiding significance for seismic design.

CONCLUSIONS

In this paper, seismic active earth pressure on retaining wall was calculated by finite element method, and the results were compared with those obtained by the pseudo-dynamic method with curved failure surface. The amplification effect of acceleration amplitude and its causes were studied, and the input seismic acceleration by pseudo-dynamic method was modified according to the characteristics of amplification effect obtained by numerical analysis. Finally, the result of the distribution of seismic active earth pressure calculated by modified pseudo-dynamic method was compared with finite element method, pseudo-static method (M-O method, Okabe (1924) and Mononobe and Matsuo (1929)) and Choudhury- Nimbalkar (2006) method. The main conclusions are as follows:

- The input seismic acceleration has obvious amplification effect in backfill along the depth of the retaining wall, which is related to many factors. Under the action of low-frequency seismic loads (f <5Hz), linear distributions of amplification factors are generated, while under the action of high-frequency seismic loads (f >5Hz), nonlinear distributions of amplification factors are generated;
- The height of retaining wall is an important factor affecting the amplification effect. The higher the retaining wall is, the more obvious the soil vibration amplification effect is and the larger the amplification factor is. In finite element numerical analysis, when other values of the parameters are certain, the amplitude of the input seismic acceleration has no obvious influence on the amplification effect.
- Based on the finite element numerical simulation results, the linear and nonlinear distributions of amplification factors were fitted mathematically. And a modified pseudo-dynamic method

was used to calculate seismic active earth pressure on the retaining wall, and the results were compared with those obtained by other methods, which were: As for total earth thrust, pseudo-static method> FE method > C-N method > modified pseudo-dynamic method; In terms of the position of action point, FE method > modified pseudo-dynamic method > C-N method > pseudo-static method.

Acknowledgements: This work was supported by the National Natural Science Foundation of China [grant number 41772275] and the Fundamental Research Funds for the Central Universities [grant number 300102268203].

References

Basha, B.M. and Babu, G.L.S. (2009) Computation of sliding displacements of bridge abutments by pseudo-dynamic method. Soil Dynam. Earthquake Engg., v.29(1), pp.103-120.

Basha, B.M. and Babu, S.G. (2009) Seismic stability analysis of reinforced soil structures using pseudo-static method. Civil Engg., v.1, pp.1389-1399.

Basha, B.M. and Babu, G.L.S. (2010) Reliability assessment of internal stability of reinforced soil structures: a pseudo-dynamic approach. Soil Dynam. Earthquake Engg., v.30(5), pp.336-353.

Basha, B.M. and Babu, G.L.S. (2010) Seismic rotational displacements of gravity walls by pseudodynamic method with curved rupture surface. Internat. Jour. Geomech., v.10(3), pp.93-105.

Bellezza and Ivo (2015) Seismic active earth pressure on walls using a new pseudo-dynamic approach. Geotech, Geol, Engg., v.33(4), pp.795-812.

Choudhury, D. and Nimbalkar, S.S. (2006) Pseudo-dynamic approach of seismic active earth pressure behind retaining wall. Geotech, Geol, Engg., v.24(5), pp.1103-1113.

Choudhury, D., Sitharam, T. and Rao, S.K. (2004) Seismic design of earth-retaining structures and foundations. Curr. Sci, v.87(87), pp.1417-1425.

Ghosh, S. (2010) Pseudo-dynamic active force and pressure behind battered retaining wall supporting inclined backfill. Soil Dynam. Earthquake Engg., v.30(11), pp.1226–1232.

Ghosh, S. and Sharma, R.P. (2012) Pseudo-dynamic evaluation of passive response on the back of a retaining wall supporting *c*-Ö backfill. Geomech. Geoengg., v.7(2), pp.115-121.

Jo et al. (2017) Evaluation of the seismic earth pressure for inverted T-shape stiff retaining wall in cohesionless soils via dynamic centrifuge. Soil Dynamics & Earthquake Engineering Southampton.

Junied, Bakr, and Mohd, A.S. (2018) A finite element performance-based approach to correlate movement of a rigid retaining wall with seismic earth pressure. Soil Dynam. Earthquake Engg., v.114, pp.460-479.

Kramer Steven (1996) Geotechnical Earthquake Engineering. Prentice Hall.

Maskar A.D., Madhekar S.N. and Phatak D.R. (2017) Redistribution principle approach for evaluation of seismic active earth pressure behind retaining wall. Jour. Institution of Engineers (India): Series A.

Miriano, Chiara, Cattoni, E. and Tamagnini, C. (2016) Advanced numerical modeling of seismic response of a propped r.c. diaphragm wall. Acta Geotechnica, v.11(1), pp.161-175.

Mononobe, N. and Matsuo, H. (1929) On the determination of earth pressures during earthquakes. Proceedings, World Engineering Congress, Vol. 9, International Association for Earthquake Engineering, Tokyo, Paper No. 388, pp.177–185.

Nakamura and Shinya (2006) Reexamination of Mononobe-Okabe theory of gravity retaining walls using cetrifuge model tests. Soils and Foundations, v.46(2), pp.135-146.

Okabe, S. (1924) General theory of earth pressure and seismic stability of retaining wall and dam. Jour. Japanese Soc. Civil Engineers, v.10(6), pp.1277–1323.

Okamura, Mitsu, and O. Matsuo (2002) A Displacement Prediction Method for Retaining Walls under Seismic Loading. Soils & Foundations, v.42(1), pp.131-138.

Rajesh, B.G. and Choudhury, D. (2017) Generalized seismic active thrust on a retaining wall with submerged backfill using a modified pseudodynamic method. Internat. Jour. Geomechan., 06016023.

Santhoshkumar, G., Ghosh, P. and Murakami, A. (2019) Seismic active resistance of a tilted cantilever retaining wall considering adaptive failure mechanism. Internat. Jour. Geomech., v.19(8), 04019086.

Seed, H. Bolton and Whitman Robert, V. (1970) Design of Earth Retaining Structures for Dynamic Loads.

Soubra and Abdul-Hamid (2001) Static and seismic passive earth pressure coefficients on rigid retaining structures. Canadian Geotech. Jour., v.7(2), pp.463-478.

Steedman, R.S. and Zeng, X. (1990) The influence of phase on the calculation of pseudo-static earth pressure on a retaining wall. Géotechnique, v.40(1), pp.103-112.

Subba Rao, K.S. and Choudhury, D. (2005) Seismic passive earth pressures in soils. Jour. Geotech. Geoenviron. Engg., v.131(1): pp.131-135.

Tavakoli, Hamidreza, Kutanaei, S.S. and Hosseini, S.H. (2019) Assessment of seismic amplification factor of excavation with support system. Earthquake Engineering and Engineering Vibration, v.3.

Terzaghi, K.T. (1943) Theoretical Soil Mechanics. INC.

Xu, Shi Yu, Shamsabadi, A. and Taciroglu, E. (2015) Evaluation of active and passive seismic earth pressures considering internal friction and cohesion. Soil Dynam. Earthquake Engg., v.70, pp.30-47.

Yan, et al. (2020) A Pseudodynamic Approach of Seismic Active Pressure on Retaining Walls Based on a Curved Rupture Surface. Mathematical Problems in Engineering, v.5, pp.1-8.

Zeng, X. and Steedman, R.S. (1993) On the behaviour of quay walls in earthquakes. Géotechnique, v.43(3), pp.417-431.